



In-Situ Observation of the Effect of the Tribofilm Growth on Scuffing in Rolling-Sliding Contact

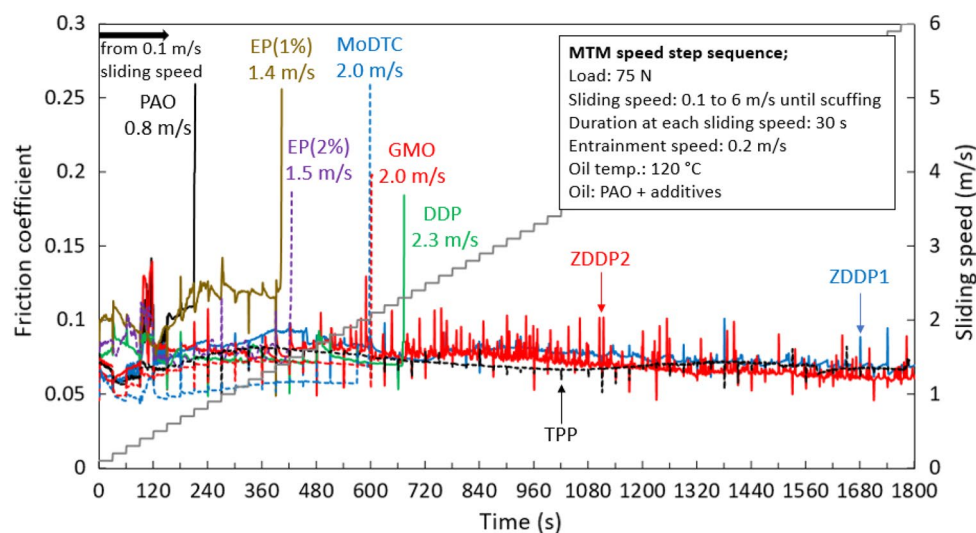
Mao Ueda¹ · Hugh Spikes² · Amir Kadiric²

Received: 16 February 2022 / Accepted: 20 May 2022 / Published online: 9 June 2022
 © The Author(s) 2022

Abstract

General reductions in lubricant viscosities in many machine components mean that the role of lubricant additives in forming tribofilms has become increasingly important to provide adequate surface protection against scuffing. However, the relationship between scuffing and the formation and removal of tribofilms has not been systematically demonstrated. In this study, a step-sliding speed scuffing test based on contra-rotation using MTM-SLIM and ETM-SLIM has been employed to observe concurrently tribofilm thickness and the onset of scuffing. The initial sliding speed used was found to significantly affect scuffing performance since it determines the extent to which a tribofilm can form before critical sliding speed conditions are reached. In general, additives that formed thicker tribofilms, especially ZDDPs and triphenyl phosphate, gave effective protection against scuffing, though their protective tribofilms were progressively removed at higher sliding speeds, eventually resulting in scuffing.

Graphical Abstract



Keywords Scuffing · Tribofilm · ZDDP · MTM

✉ Mao Ueda
 m.ueda@shell.com

¹ Technology Centre, Shell Lubricants Japan K.K., Tokyo, Japan

² Tribology Group, Imperial College London, London, UK

1 General Introduction

Scuffing has been defined as “gross damage characterised by the formation of local welds between sliding surfaces” [1] and is a recurrent problem in heavily loaded, high sliding speed contacts as present in gears, sliding cam-followers and

some roller bearings. It originates from local breakdown of the fluid film and any tribofilms that separate the rubbing surfaces in response to a change in contact conditions, such as an increase in operating load, speed or temperature, or entry of solid contamination particles into the contact. This leads to a sudden increase in asperity friction and, thus, to a rise in surface temperature and surface damage, both of which, in high sliding conditions, precipitate a catastrophic collapse of the lubricating film across the whole contact. Various mechanisms that lead to the onset and progression of scuffing have been proposed, but it is still not clear which of these is most influential in practice [2].

In recent years, the need to improve energy efficiency has led to both an increase in power densities of components in many applications and to their being lubricated by lower viscosity oils to reduce hydrodynamic friction and churning. Both these trends mean that scuffing is becoming more prevalent and of increasing concern to lubricant formulators [3]. Scuffing has also been identified as a likely problem in high-speed electric vehicle transmissions [4].

For scuffing to occur, both the elastohydrodynamic (EHL) film and any protective tribofilms present on the surfaces must break down, resulting in direct metal-metal contact and adhesion [5, 6]. The conditions that lead to the breakdown of EHL films have been quite extensively studied [7] and form the basis for several important predictive scuffing models based on critical temperature and related PV (load/sliding speed) criteria [8, 9]. Our understanding of the impact of tribofilm formation and removal on scuffing is much less developed, though it is evident that such tribofilms formed by extreme-pressure (EP) and antiwear additives can play a very important role in scuffing control; indeed, sulphur-based EP additives were originally developed expressly to prevent scuffing of hypoid gears [10]. Historically, most EP additives were based on organochlorine and organo-sulphur compounds [10], but halogen-based additives are no longer used for environmental reasons. Sulphur-free, organophosphorus-based additives are generally considered primarily as antiwear additives but have also been recognised to possess EP properties [10].

Using a four-ball tester, Piekoszewski et al. [11] showed that tribofilms formed by ZDDP and S/P EP solutions improved scuffing performance, while Yamamoto et al. [12] used a Timken roller on ring tester to show that aryl phosphates were more effective as extreme-pressure agents than alkyl phosphates. They attributed this to the aryl type being able to form more protective tribofilms. Palacios [13] applied EDX after a four-ball test to show that ZDDP tribofilm thickness increased as load increased, before becoming progressively thinner to eventually give scuffing at very high load. Miyajima et al. [14] studied the role of EP additive in controlling scuffing alongside in situ observation of tribofilm development using a Raman tribometer. The authors used

a starved contact to induce scuffing and showed that FeS₂ tribofilm formed initially, and this then thinned as rubbing progressed, to eventually give scuffing. After scuffing, no FeS₂ tribofilm remained on the surfaces. A similar response to Miyajima's was observed using a MTM-SLIM in contra-rotation mode [15–17]. Bayat et al. [16] suggested that, while parts of tribofilms were removed from surfaces after micro-scuffing, this did not propagate to catastrophic scuffing until a critical sliding speed was reached at which tribofilms could not form quickly enough on exposed surfaces. The term *micro-scuffing* refers to local scuffing that does not persist or spread over the whole surfaces and is characterised by a sudden rise and then quick fall of friction coefficient [6, 15, 18–20]. As well as antiwear additives and EP additives, Ingram et al. [17] showed that a long-chain amide type of friction modifier improved scuffing performance.

From the above, it is evident that some lubricant additives form protective tribofilms that play an important role in protecting surfaces from scuffing. However, the mechanisms by which the evolution of such tribofilms affect scuffing are still poorly understood. Therefore, this paper aims to understand the effect of various lubricant additives on the development of tribofilms at the same time as measuring their effect on scuffing. Since scuffing is likely to occur in gears, bearings and sliding cam-followers, additives used to lubricate such components were studied, including antiwear additives, EP additives and friction modifiers. Scuffing was obtained using MTM/ETM ball-on-disc tribometers in contra-rotation mode with SLIM for simultaneous observation of the evolution of tribofilm on the ball. The influence of running-in was explored to assess the importance of forming a tribofilm prior to the critical sliding speed to give scuffing. The results obtained provide practical insight into the formulation of lubricants with anti-scuffing performance and some understanding of the relevant mechanisms by which lubricant additives mitigate scuffing.

2 Scuffing Test Methodology

2.1 Introduction

Scuffing performance has been measured using many different experimental techniques including the four ball [11], block on ring [21], Amsler [22], Ryder [23], IAE [24] and FZG [9]. Some of these tests employ pure sliding conditions [11, 21] and others mixed rolling-sliding [9, 23, 24]. These techniques have several problems for studying scuffing as discussed in some detail by Peng et al. [15]. In pure sliding tests, one of the contacting bodies is stationary, so that a single location on its surface is always in contact with the counterface. This location experiences cumulative mild wear that increases the contact area and,

hence, reduces the contact pressure prior to scuffing. This can lead to misinterpretation of anti-scuffing performance since a test oil with poor antiwear performance may show good scuffing prevention simply because the rubbing surfaces wear extensively to give very low contact pressure. This problem can be mitigated using rolling-sliding rigs such as disc and gear machines in which, because both surfaces move with respect to the contact, mild wear is distributed over the wear tracks on surfaces, i.e. there is no continuous wear at a single contact point.

A second problem is that almost all scuffing tests are based on increasing the applied load in stages until scuffing occurs, a so-called *step-load* sequence [25]. This sequence introduces unworn, fresh surface into contact when the contact area is enlarged due to increased load and the resulting contact of fresh, unprotected asperities can precipitate scuffing [19]. This can lead to misunderstanding of lubricant performance since scuffing can occur due to unprotected fresh surface at high load regardless of the ability of the lubricant to form tribofilms. To address this problem, a *step-speed* protocol could be used in which sliding speed is increased at constant load during a test. Because load does not increase, no fresh surface comes into contact. However, it is impossible to increase sliding without also increasing entrainment speed in pure sliding tests and difficult to do so in gear-based testers such as the Ryder, IAE and FZG since gear geometry alone establishes the ratio between sliding and entrainment speed. Entrainment speed controls the extent to which oil is dragged into the contact, and thus, the EHL oil film thickness and this itself will strongly influence the tendency to scuff.

A third problem in some scuffing tests such as the four-ball scuffing test is that they are too short to enable the formation of tribofilms, so that what is measured is the ability of a lubricant to provide almost instantaneous surface protection rather than that of a well run-in surface. The

main concern in most practical applications, however, is to prevent scuffing from occurring during machine operation, not during running-in. This limitation was recognised by Perez et al. who proposed a four-ball scuffing test that was preceded by a prolonged running-in stage [25]. This issue will be considered in the current paper by examining various running-in conditions.

To address all the above problems, Ingram et al. [17] employed a ball-on-disc machine (MTM) to provide a rolling-sliding contact that could operate in contra-rotation mode, i.e. in which a ball and a disc could rotate in opposite directions. This allowed a very wide range of sliding speeds to be obtained at fixed entrainment speed and, thus, made possible a step-speed test sequence. Ingram's method, and especially its running-in stage, was recently modified by Peng et al. [15] to obtain better repeatability of scuffing by added a short rubbing stage at low load and low sliding speed to smooth the surfaces before the main step-speed test sequence. Very recently, using a barrel on disc MTM set-up, Bayat et al. [16] have developed this approach further to better study additive performance by starting the main step-speed sequence at lower sliding speed but the same load as the main test sequence. This enables tribofilm coverage to develop over the whole contact area subsequently present in the main step-speed sequence.

2.2 Experimental Equipment

All scuffing tests were carried out using a similar method to that employed by Peng et al. [15]. A mini-traction machine (MTM) and an extreme-traction machine (ETM), both with spacer layer imaging attachments (SLIM) were employed to generate scuffing and to monitor tribofilm development. MTM and ETM are ball-on-disc tribometers with a similar configuration, as shown schematically in Fig. 1 and were supplied by PCS Instruments, UK. The main difference between the two is that the ETM can reach much higher applied loads and, thus, contact pressures than the MTM. In both machines, a ball is loaded against the flat surface of a steel disc immersed in lubricant. The ball and the disc are driven by separate electric motors at user-specified rolling/sliding conditions. To capture SLIM images, the rubbing

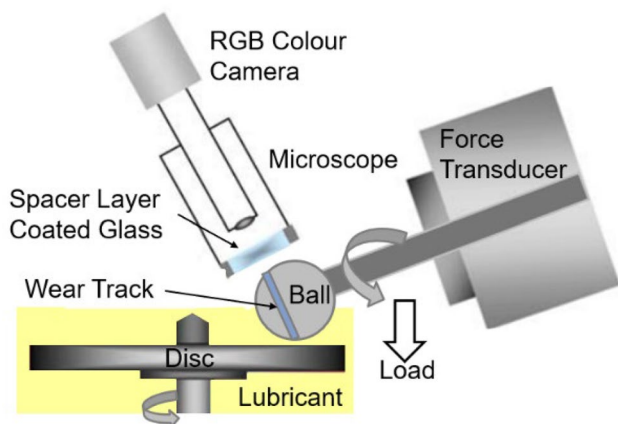


Fig. 1 Schematic image of MTM-SLIM and ETM-SLIM

Table 1 Properties of MTM and ETM specimens

	Ball	Disc
Material	AISI 52100 steel	AISI 52100 steel
Elastic modulus (GPa)	207	207
Poisson's ratio	0.3	0.3
Vickers hardness (H_v)	820 ± 30	730 ± 30
Roughness, R_q (nm)	7 ± 2	9 ± 3
Diameter (mm)	19.05	46

test is paused periodically and the ball is raised and loaded against a glass flat coated with a semi-reflective chromium layer and a transparent silica space layer. Light reflected from the chromium layer and the ball surface undergo optical interference upon recombination, generating an interference image of the contact between the ball and the coated glass surface that is captured by an RGB camera. Tribofilm thickness is calculated from this interferometric image using calibrated RGB values. Table 1 lists the properties of MTM and ETM specimens used in this study. A 19.05-mm-diameter AISI 52100 steel ball and a 46-mm-diameter AISI 52100 disc were employed and supplied by PCS Instruments. Both specimens had smooth surfaces, less than 10 nm R_q . Previous work has showed that tests on the MTM and ETM conducted at the same load (which is only possible between 40 and 75 N) gave the same scuffing performance although ETM is not designed to provide a stable load below 100 N [15].

2.3 Test Conditions

The scuffing test sequence employed in this study is based on previous MTM-based scuffing work [15–17]. After a running-in stage at very low entrainment speed, the load and entrainment speed are held constant while the sliding speed is increased in steps at constant entrainment speed and applied load until scuffing occurs. The entrainment speed

is defined by $U = (u_{\text{disc}} + u_{\text{ball}})/2$ while the sliding speed $U_s = (u_{\text{disc}} - u_{\text{ball}})$, where u_{ball} and u_{disc} are the velocities of the ball and disc surface with respect to the contact. The slide-roll ratio, SRR is the ratio of the sliding speed to the entrainment speed.

To enable sliding speeds greater than twice the entrainment speed, as is the case when one surface is stationary with respect to the contact, the MTM is operated in contra-rotation mode, with the ball and disc rotating in opposite directions with respect to the contact so that u_{ball} and u_{disc} have opposite signs. This enables sliding speeds up to 6 m/s to be reached even at low entrainment speed. Between each speed-step stages in the test sequence, there is a rest stage where the ball and disc are rotated at zero applied load to enable the surfaces to cool. At the start of each rest stage, a SLIM interference image is obtained to determine the presence and thickness of any tribofilm on the ball surface. Figure 2 shows a schematic image of the various stages in each scuffing test while Table 2 shows the conditions used in each stage.

The above scuffing test sequence was carried out at five applied loads, 20 N, 40 N and 75 N in the MTM, and 210 N and 570 N in the ETM. These loads correspond to 0.8 GPa, 1.0 GPa, 1.3 GPa, 1.8 GPa and 2.5 GPa maximum Hertzian pressure, respectively. It is important to note that separate scuffing tests were carried out at each applied load. This differs from the study by Bayat et al. [16], where, if scuffing

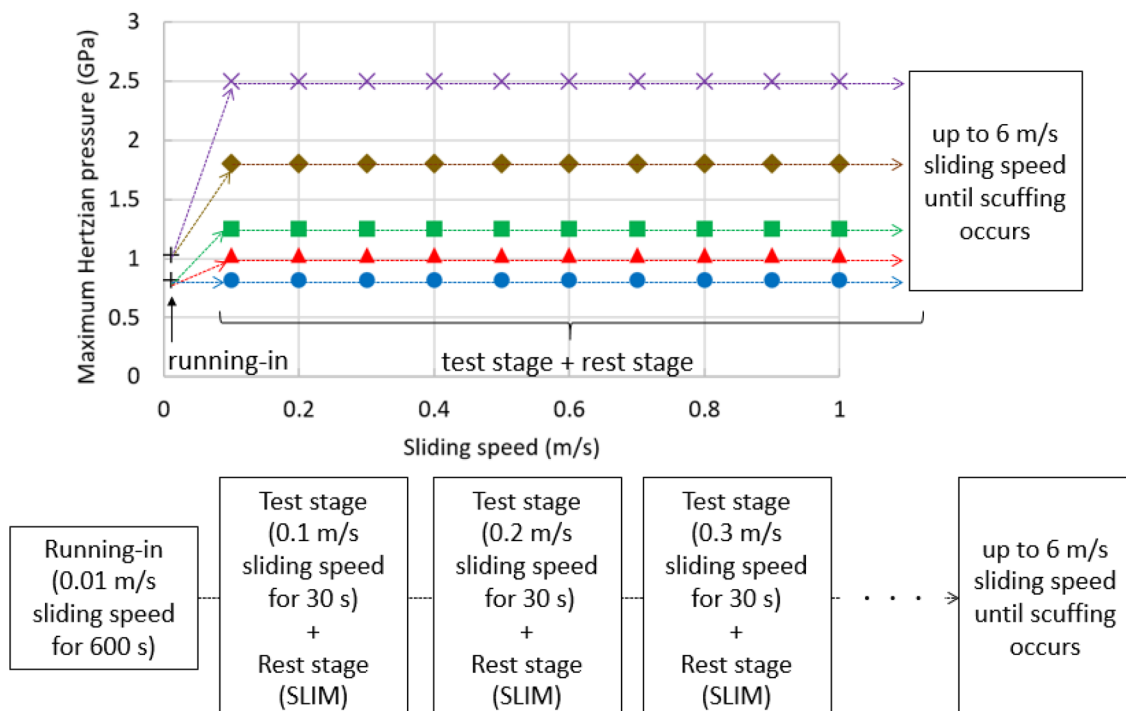


Fig. 2 The variation of the maximum Hertzian pressure and sliding speed in the scuffing tests. Each test point consists of a 30 s test stage followed by a rest stage of 30 s to capture a SLIM image. The 600 s running-in stage is denoted by a+

Table 2 Scuffing test conditions using MTM and ETM

	Running-in	Test stage	Rest stage
Test load (N) (Maximum Hertzian Pressure (GPa))	MTM: 20(0.8) ETM: 50(1.1)	MTM: 20(0.8), 40(1.0), 75(1.3) ETM: 210(1.8), 570(2.5)	Unloading the ball from the disc and loading it against a glass flat under stationary contact to capture SLIM images
Entrainment speed (m/s)	0.003	0.2	
Sliding speed (m/s)	0.01	0.1, 0.2, 0.3... 6 Test stopped when scuffing occurs	
Duration (s)	600	30	30
Test temperature (°C)	120		

was not observed at the first applied load of 20 N, the same series of sliding steps sequence was repeated at higher and higher loads until scuffing eventually occurred. In the current study, all tests were carried out at 120 °C and each combination of lubricant and load was tested at least twice to verify repeatability.

2.3.1 Running-in stage

It is widely accepted that the distribution of asperity heights is very critical to scuffing [19] and to eliminate variations in roughness prior to the main test sequence, previous studies have suggested an initial running-in stage at very low sliding and entrainment speed and low load [15–17]. In the current study, the same 600 s running-in stage as developed by Peng [14] was employed, with a very low entrainment speed of 3 mm/s and a sliding speed of 0.01 m/s. These conditions are designed to give negligible EHD film thickness to ensure a lot of asperity contact but with little sliding to limit adhesive damage. The applied load was 20 N for the MTM and 50 N for ETM. A higher load was applied in the ETM tests because the latter is not designed to provide a stable load below this value.

2.3.2 Step-Speed Stages

After the running-in stage, the main step-speed sequence was carried out. Each sliding speed stage lasted 30 s during which the entrainment speed was held constant at 0.2 m/s. In most tests, this sequence started from an initial sliding speed of 0.1 m/s, and this was increased in increments of 0.1 m/s until scuffing occurred or the maximum possible sliding speed value of 6 m/s was reached. However, in some tests as described below, the initial sliding speed was varied to determine the impact of this on scuffing. Scuffing was recognised by a sudden and permanent increase of a friction accompanied loud noise and strong vibration, and when this occurred, the test was manually halted.

2.3.3 Rest Stages

Each step-speed stage was followed immediately by 30 s rest stage. In this, the ball is unloaded from the disc and loading it against a glass flat under stationary contact in order to acquire a coloured interference from which to determine any tribofilm thickness (SLIM) [26]. This procedure lasts 30 s during which the disc is slowly rotating in the oil bath. This rest stage had three purposes. First, it enabled an interference image to be obtained from the ball track. Second, it allowed the specimen surfaces and the bulk lubricant temperature to cool down to the set value. Frictional heating effects of both the specimens and the lubricant are significant in many conventional scuffing tests and make it difficult to define the exact conditions at the onset of scuffing [2]. Third, rotating in lubricant with no contact helps clear any debris which may be trapped or accumulated on the rubbed tracks during the test stages, which itself has been observed to be able to cause scuffing [27]. The rest stage is, therefore, an important component of the procedure to ensure that the conditions at the onset of scuffing are repeatable.

2.4 Test Lubricants

The oil formulations used in this study are listed in Table 3. To ensure thin film and, thus, boundary and mixed lubrication conditions, a polyalphaolefin (PAO) with a quite low viscosity of 18.5 mm²/s at 40 °C and 4.1 mm²/s at 100 °C was employed as base oil. Its kinematic viscosity and dynamic viscosity at the test temperature of 120 °C were 3.0 mm²/s and 2.3 cP, respectively. Additives used were anti-wear additives (two zinc dialkyldithiophosphates (ZDDPs), ashless dialkyldithiophosphate (DDP), triphenyl phosphate (TPP)), S-type extreme-pressure (EP) additive (sulphurised isobutylene) and friction modifiers (molybdenum dithiocarbamate (MoDTC) and glycerol monooleate (GMO)). These were blended individually in PAO at the concentrations shown in Table 3, concentrations typically used in gear oils and engine oils. The dosage of these additives in PAO is not high enough to significantly impact the blend viscosity so that all blends can be considered to have the same

Table 3 Test oil formulations

Lubricant name	Additive concentration	Kinematic viscosity at 40 °C/100 °C, mm ² /s
PAO	–	18.5/4.1
ZDDP1 (zinc dialkyl dithiophosphate, primary 2-ethylhexyl)	P: 800 ppm S: 1700 ppm	–
ZDDP2 (zinc dialkyl dithiophosphate, secondary C6)	P: 800 ppm S: 1700 ppm	
DDP (dithiophosphate)	P: 800 ppm S: 1700 ppm	
EP(1%) (sulphurised isobutylene)	S: 1%	
EP(2%) (sulphurised isobutylene)	S: 2%	
TPP (triphenyl phosphate)	P: 1600 ppm	
MoDTC (molybdenum dithiocarbamate)	Mo: 300 ppm S: 340 ppm	
GMO (glycerol monooleate)	GMO: 0.4 wt%	

EHD film-forming capability. At the entrainment speed of 0.2 m/s used in the main test sequence, the calculated minimum oil film thickness was 5 to 6 nm (depending on the applied load). This corresponds to an initial, theoretical lambda ratio (ratio of EHD film thickness to composite surface roughness) of 0.4 to 0.5 and, thus, to mixed lubrication conditions. In the running-in stage where the entrainment speed was 0.01 m/s, the calculated minimum oil film thickness was ca. 0.7 nm, corresponding to $\lambda = 0.06$ and, thus, to boundary lubrication conditions.

2.5 Surface Observation

Tribofilms formed on steel balls were quantified from the SLIM images obtained during each rest stage. Upon completion of each MTM and ETM test, the wear tracks of the balls and the discs were observed using an optical microscope and an optical white light interferometer (WLI, WYKO NT 9100).

3 Results

3.1 Initial Sliding Speed in the Main Test Sequence

Since this study was concerned with the influence of tribofilms on scuffing, it was important to ensure that the scuffing test protocol made it possible for a tribofilm to form on the rubbing surfaces prior to the conditions becoming severe enough to cause scuffing. The running-in stage alone was not sufficiently severe enough to ensure this, especially since its low load meant that, when a higher load was then applied, unrubbed surface was introduced to the contact. Peng et al. used an initial sliding speed of 0.6 m/s in their

main test sequence, while Bayat et al. [16] started the step-speed sequence at 0.3 m/s sliding to give more time for tribofilm to form. In the current study, the influence of initial sliding speed stage was investigated by started the main step-speed test sequence at three different sliding speeds, 0.1 m/s, 0.6 m/s and 1 m/s.

Figure 3a and b shows the variation of friction during the main step-speed sequence for PAO and ZDDP2 at 20 N when the test stages were started at three different sliding speeds after running-in. Figure 3b shows a magnified region of Fig. 3a up to 1.6 m/s sliding speed. Apart from the variation in initial sliding speed, all tests were carried out at the conditions shown in Table 2. It should be noted that the running-in and the rest stages are not shown in this and all subsequent figures. Regardless of the initial sliding speed, additive-free PAO gave a sudden friction increase characterising scuffing at around 1.0 m/s sliding speed. ZDDP2 showed no scuffing up to 6 m/s in the tests started at 0.1 m/s and 0.6 m/s sliding speed. However, when the initial sliding speed was 1.0 m/s, scuffing occurred immediately after this stage began. It should be noted that the momentary blips in the friction traces between speed steps in Fig. 3 are artefacts of the measurement method and occur just after motion is paused to capture SLIM images during the rest stages. However, variations of friction coefficient can also be seen within individual sliding step, especially for the data from ZDDP2. This may result from surface modifications such as micro-scuffing and/or partial tribofilm removal, not leading to catastrophic scuffing.

Figure 4a and b shows friction development in tests on the same two lubricants at 75 N. At this higher load, scuffing of PAO occurred slightly earlier than at 20 N, *i.e.* at 0.8 m/s and 0.7 m/s, when the tests were started from 0.1 and 0.6 m/s sliding speed, respectively. ZDDP2 showed

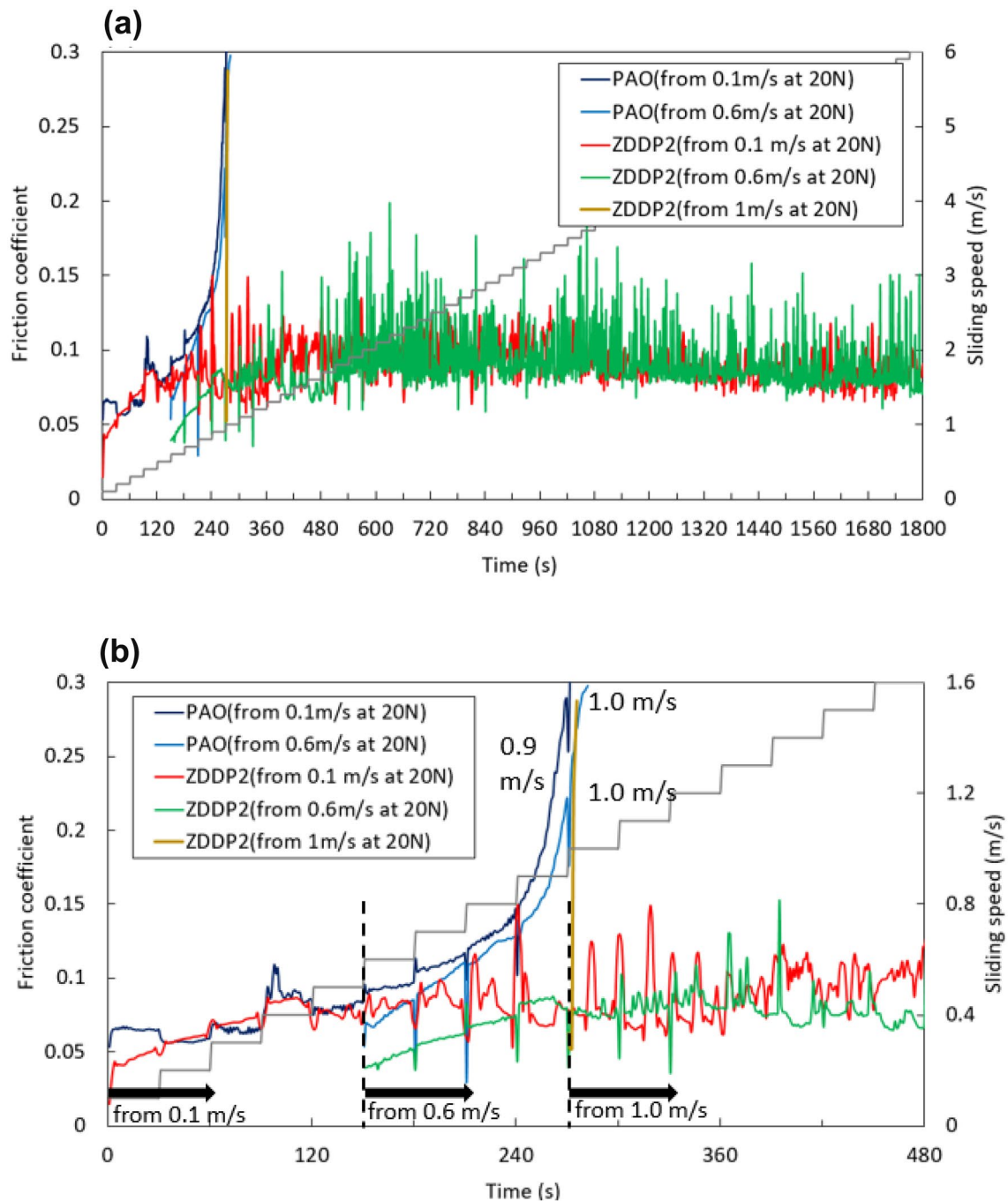


Fig. 3 The effect of initial sliding speed on friction coefficient in PAO and ZDDP2 at 20 N. **a** shows the data from 0 to 6 m/s sliding speed, while **b** focusses on the friction data between 0 and 1.6 m/s. Except

for variations in the initial sliding speed in the test stage, the tests were carried out in the condition shown in Table 2

no scuffing up to 6 m/s when the sliding speed sequence started at 0.1 m/s, as seen at 20 N load. However, scuffing occurred at 1 m/s sliding speed in tests when the initial sliding speed was both 0.6 m/s and 1 m/s.

These results show that for additive-free PAO, the sliding speed at which scuffing occurs is largely independent of the initial sliding speed used, so long as the latter is less

than the speed at which scuffing takes place. For ZDDP2 solution, however, the scuffing speed depends strongly on the speed at which the test sequence starts (Figs. 3, 4). If the test sequence starts at a high sliding speed, scuffing occurs at much lower speed than if it starts at 0.1 m/s. This is believed to result from the fact that when test stages start at low sliding speed, ZDDP2 can develop a protective

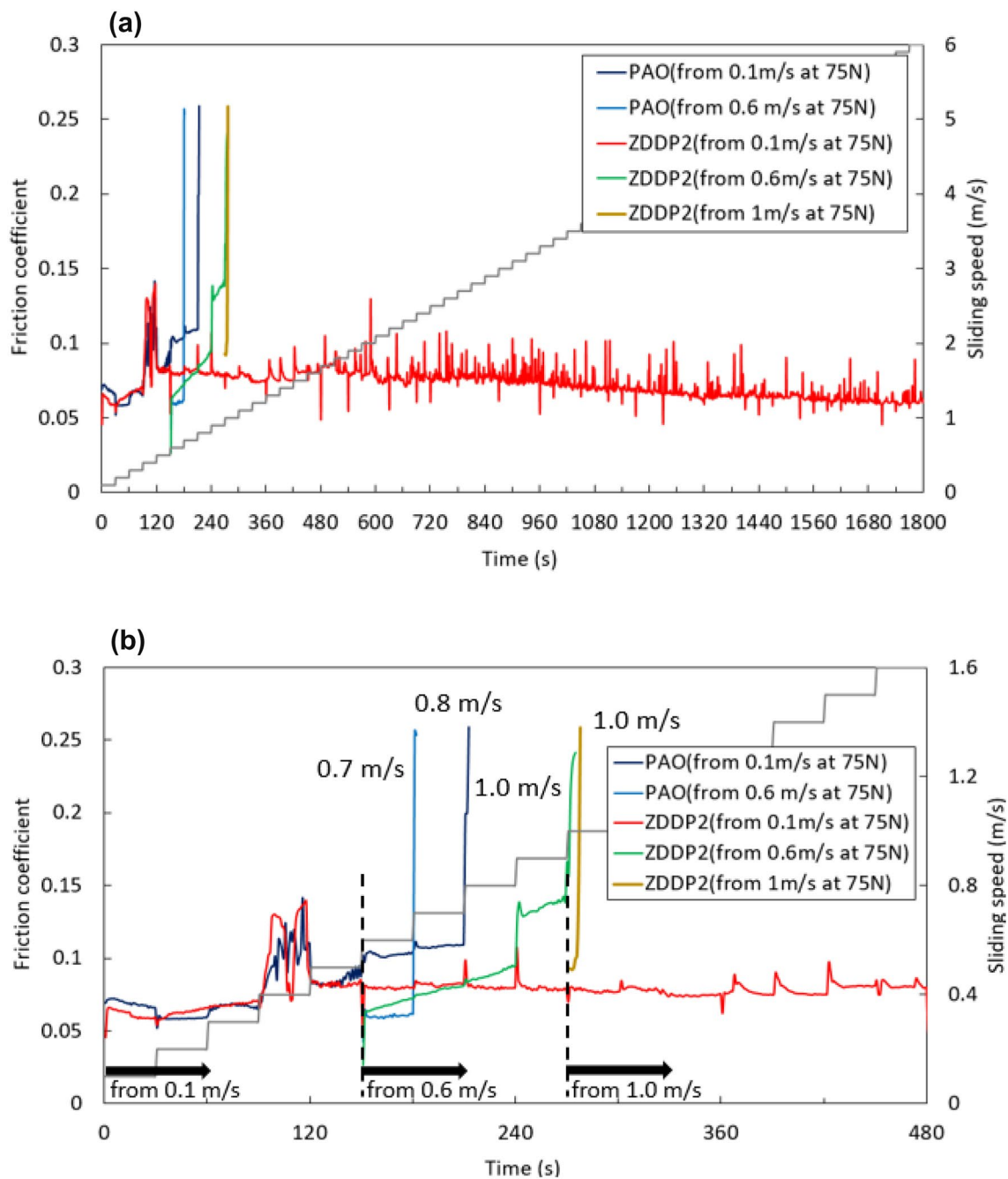


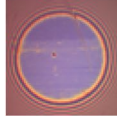

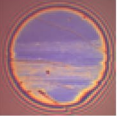

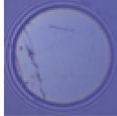


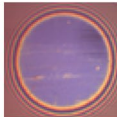




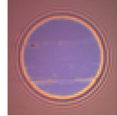
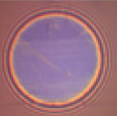

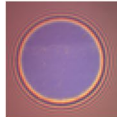
Fig. 4 The effect of initial sliding speed on friction coefficient in PAO and ZDDP2 at 75 N. **a** shows the data from 0 to 6 m/s sliding speed, while **b** focusses on the friction data between 0 and 1.6 m/s. Except

for variations in the initial sliding speed in the test stage, the tests were carried out in the condition shown in Table 2

tribofilm in the early speed stages and this then provides protection against scuffing at intermediate sliding speeds. Figure 5 shows SLIM images and mean tribofilm thickness obtained after the running-in stage and after test stages at 0.1, 0.6 and 0.9 m/s from separate tests starting at sliding speeds of 0.1, 0.6 and 1 m/s. When the tests started from 0.1 m/s sliding speed, ZDDP2 formed more than twice the tribofilm thickness after the 0.6 m/s and 0.9 m/s stages at

both 20 N and 75 N than when the tests started at 0.6 m/s. These relatively thick tribofilm could then protect against scuffing at sliding speeds when scuffing would occur in the absence of effective tribofilm (e.g. in PAO alone), i.e. at around 1 m/s of sliding speed. This result also suggests that the thickness of tribofilm needed to protect surfaces from scuffing is dependent on applied load, i.e. scuffing is avoided with a thinner tribofilm at lower load. When tests

Fig. 5 The effect of initial sliding speed on tribofilm development of ZDDP2 at 20 N and 75 N. SLIM images after running-in and the given test stage are shown

		after running-in	after 0.1 m/s for 30 s	after 0.6 m/s for 30 s	after 0.9 m/s for 30 s
20 N	from 0.1 m/s	 4 nm	 6 nm	 9 nm	 12 nm
	from 0.6 m/s	 2 nm	-	 3 nm	 6 nm
	from 1 m/s	 2 nm	-	-	-
75 N	from 0.1 m/s	 3 nm	 3 nm	 7 nm	 12 nm
	from 0.6 m/s	 2 nm	-	 3 nm	 5 nm
	from 1 m/s	 2 nm	-	-	-

were started from 1.0 m/s sliding, 2–3 nm of tribofilm was present after the running-in, but this was too thin to prevent immediate scuffing.

This result suggests that the initial sliding speed of the test stage significantly affects scuffing performance for lubricants containing tribofilm-forming additives. Therefore, all further scuffing tests in this study started the step-speed test sequence at 0.1 m/s sliding speed.

3.2 Effect of Load in Running-in Stage on Scuffing

Instead of varying the initial sliding speed, another way to allow tribofilms to form prior to step-speed testing would be to promote tribofilm formation during the running-in stage, i.e. use a higher load and/or a longer duration in this stage. To understand the effect of running-in on tribofilm

formation and subsequent scuffing, three different running-in conditions were compared, 50 N for 600 s and 50 N for 3600 s in addition to the default condition of 20 N for 600 s. After running-in, the test stages were then started from 0.6 m/s sliding speed at 75 N to compare the sliding speed at which scuffing occurred.

Figure 6 compares the development of friction coefficient at 75 N after running-in at the three different conditions. Running-in at 20 N for 600 s, the default condition, led to scuffing at the 1 m/s sliding speed stage. Surprisingly, running-in at 50 N for 600 s and 50 N for 3600 s gave scuffing at almost the same sliding speed.

To understand the reason for this, the development of tribofilm was investigated. Figure 7 shows optical micrographs and SLIM images of the balls immediately after the running-in in the three above conditions and also after

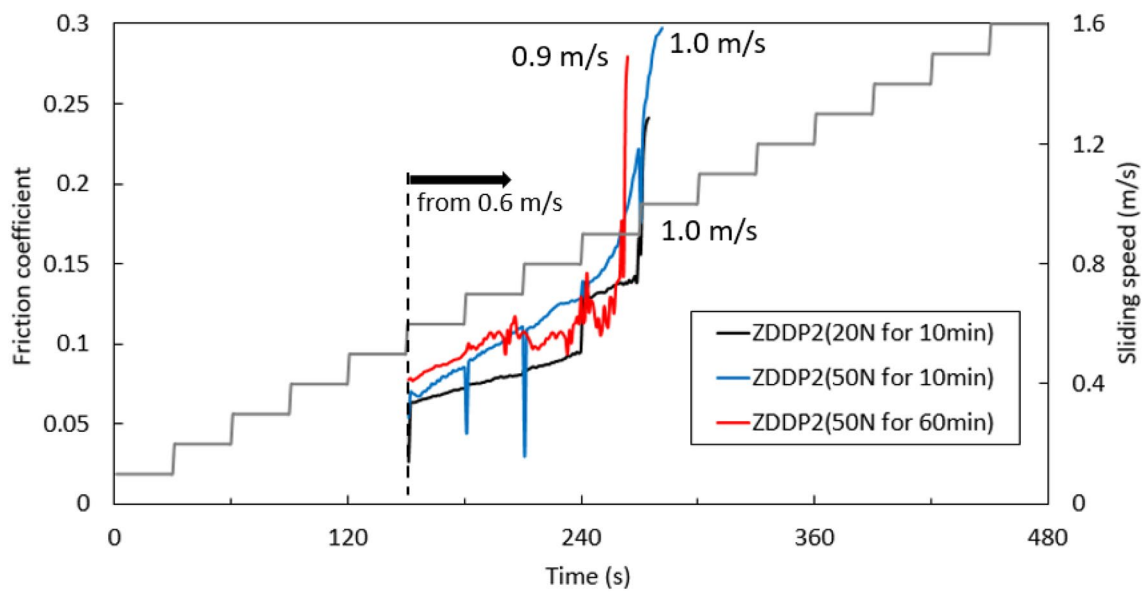


Fig. 6 The effect of load and duration of the running-in stage on friction coefficient in the subsequent 75 N test sequence. Note that the initial test stage in the test sequence was 0.6 m/s


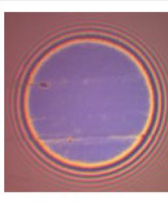
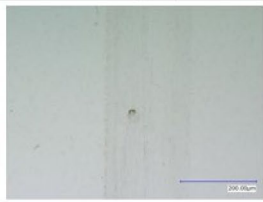
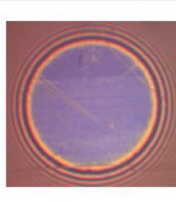
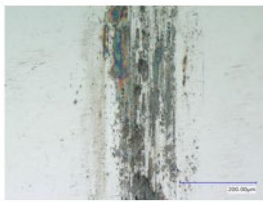


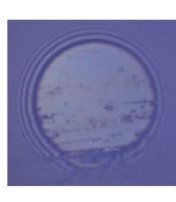
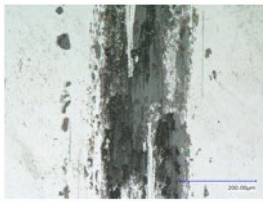
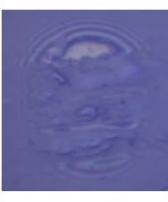
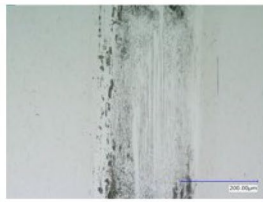
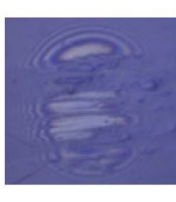
	After running-in		After 30 s sliding at 0.6 m/s	
	micrograph	SLIM image	micrograph	SLIM image
20 N, 600 s running-in				
50 N, 600 s running-in				
50 N, 3600 s running-in				

Fig. 7 The effect of load and duration in the running-in on the ball surfaces. Optical micrographs of the balls and SLIM images after the running-in stage and after the initial test stage at 0.6 m/s and

75 N (Note the scale bar included in the top-left images of the figure applies to all images)

the initial test stage at 0.6 m/s sliding speed. These images show that when running-in load increased from 20 to 50 N and also when the running-in duration was extended from 600 to 3600 s, a thicker tribofilm was formed. However,

when these tribofilms were rubbed in the initial 0.6 m/s sliding speed test stage, most of these thick tribofilms were removed. Consequently, no protective tribofilm survived prevent scuffing at around 1 m/s sliding speed.

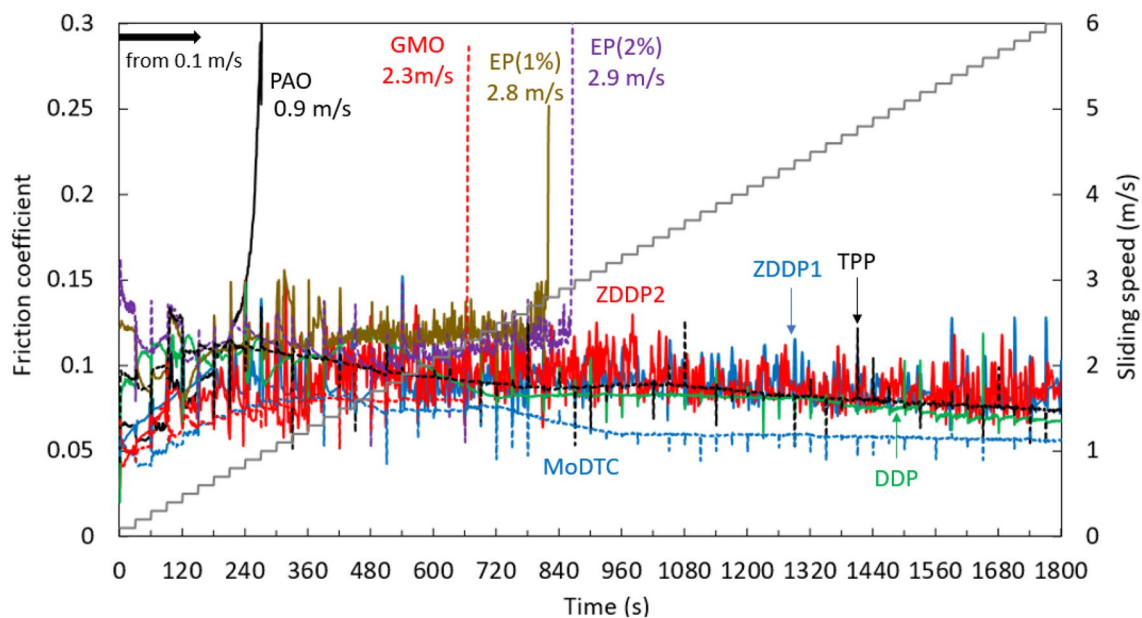


Fig. 8 The development of friction coefficient during the test stages at 20 N in nine lubricants. Tests were carried out at the condition shown in Table 2

Scrutiny of the ZDDP tribofilms formed after the high load and long duration running-in stages showed that these tribofilms had a glassy appearance, formed only on some parts of the wear tracks and consisted of large, relatively smooth lumps, rather than the fine, pad structure seen in many previous studies [28]. A previous study has shown that when ZDDP tribofilms form, they initially have a predominantly amorphous polyphosphate structure, and these polyphosphates are easily removed by rubbing in a base oil [29, 30]. It was also reported that ZDDP tribofilms having a glassy appearance formed on $\text{Si}_3\text{N}_4/\text{Si}_3\text{N}_4$ were completely removed after rubbing in a base oil [31]. Possibly, the tribofilms formed after the high load and long duration running-in stages have such characteristics and are, thus, easily removed.

Based on the above results, the running-in conditions developed by Peng et al. [15] were used in this study but combined with an initial test stage at 0.1 m/s sliding speed.

3.3 Effect of Lubricant Additives on Scuffing

In this section, the effect of different lubricant additives on both scuffing and tribofilm development are described. The test protocol is as shown in Table 2. Results at three loads, 20 N, 75 N and 570 N are described in detail.

3.3.1 Scuffing Behaviour at 20 N

Figure 8 shows how friction coefficient varied in the test sequences at 20 N for all nine lubricants listed in Table 3. Additive-free PAO scuffed at the 0.9 m/s test stage and all 8 additives extended this scuffing speed performance. EP(1%), EP(2%) and GMO scuffed at the 2.8 m/s, 2.9 m/s and 2.3 m/s sliding speed stages, respectively. By contrast, ZDDP1, ZDDP2, DDP, TPP and MoDTC did not show any scuffing up to the highest attainable sliding speed stage of 6 m/s. It is interesting to note that the S-based EP additive showed scuffing, while the P-S-based AW/EP additives did not scuff at this load.

There are noteworthy differences between the friction traces of the various additive solutions. Even though the two ZDDP solutions did not scuff, their friction traces fluctuated markedly through the tests, much more than the other additive solutions, in particular DDP, TPP and MoDTC. MoDTC and GMO gave lower friction coefficients than other formulations; i.e. 0.08 at 1.5 m/s while the other lubricants all showed friction coefficients over 0.1 at this sliding speed. MoDTC showed no scuffing at 20 N, but GMO scuffed at 2.3 m/s sliding speed.

Figure 9 shows the evolution of tribofilm thickness of lubricants during the test stages at 20 N. The values shown at 0 s are tribofilm thicknesses after the running-in stage. The lubricants that gave scuffing, i.e. EP(1%), EP(2%) and GMO, formed relatively thin films in the test stages, all less than 8 nm. These films may be too thin to prevent scuffing.

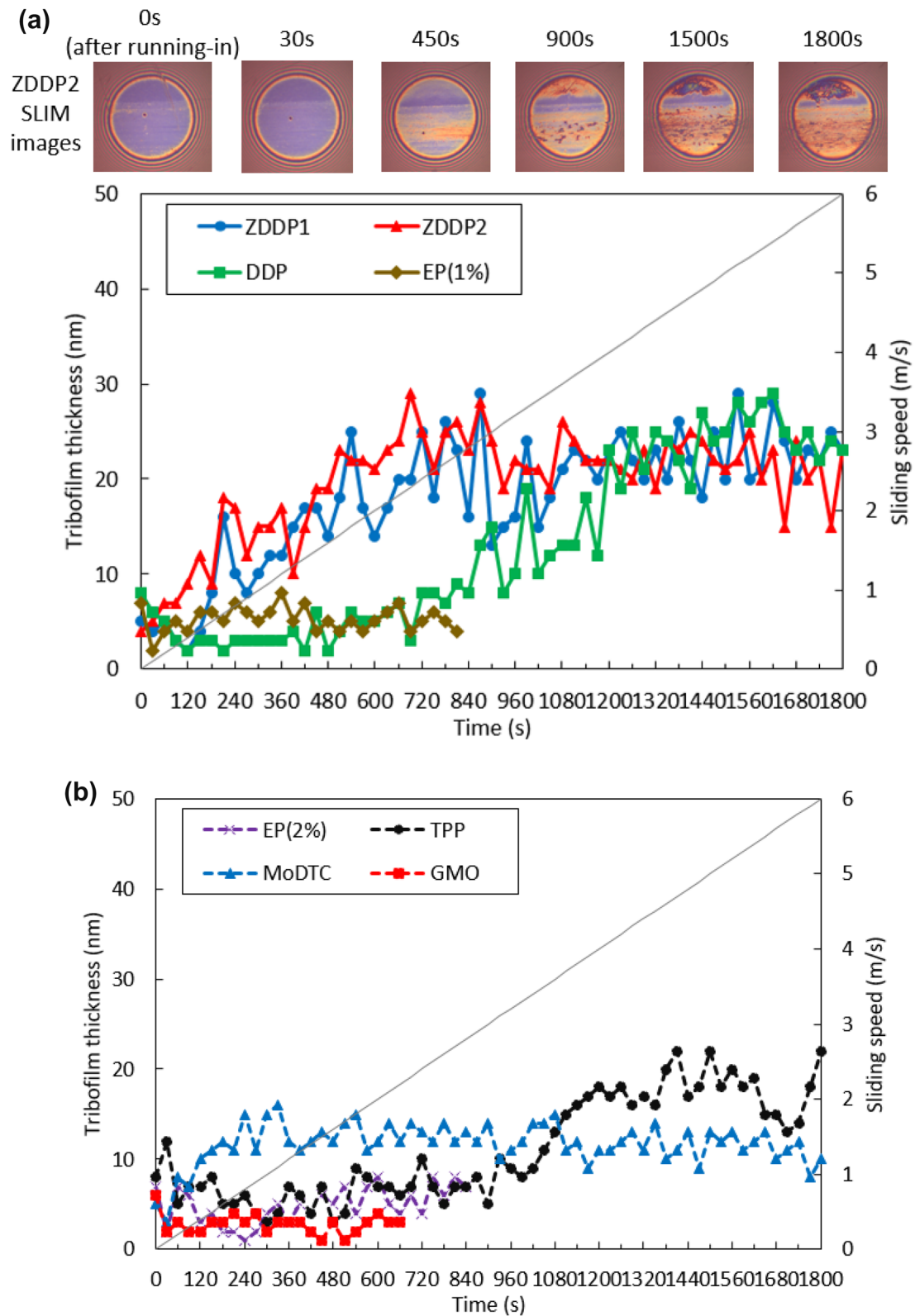


Fig. 9 The development of tribofilm thickness formed by various lubricants at 20 N as quantified by SLIM images captured during the rest stages. SLIM images of ZDDP2 at given durations are also shown in **a**

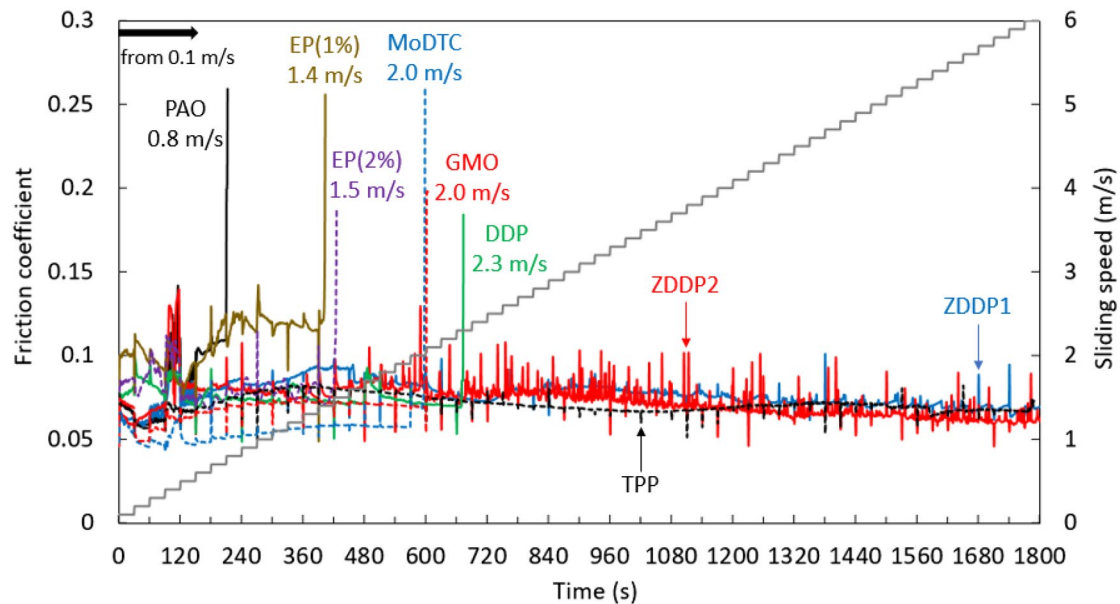


Fig. 10 The development of friction coefficient during the test stages at 75 N in the nine lubricants. Tests were carried out at the conditions shown in Table 2

Interestingly, up to the 3 m/s test stage, DDP and TPP formed relatively thin tribofilms of less than 10 nm, but their film thicknesses then grew to more than 20 nm above this sliding speed stage. It has been shown that these ashless P-S additives form films more slowly than ZDDPs [32]. MoDTC formed a thick tribofilm of around 10 nm to 15 nm quite early in the test sequence and this remained stable up to 6 m/s.

ZDDP1 and ZDDP2 formed relatively thick, 15 to 30 nm, tribofilms very rapidly, to stabilise at around 20 nm up to the highest speed stage. As much research has reported, since ZDDPs form relatively patchy and thick tribofilms, they increase friction in mixed lubrication conditions due to the formation of a rough, solid tribofilm surface that reduces fluid entrainment [33, 34]. Based on the variation of tribofilm thickness of ZDDP1 and ZDDP2, it appears that partial formation and removal of tribofilm may be continuously occurring. This might also result in the observed fluctuations of friction coefficient. From SLIM images of ZDDP2 shown in Fig. 9a, the initial circular contact does not become significantly distorted during the test stage, which indicates that significant wear that might lower contact pressure was not occurring. This retention of contact circularity was seen in all lubricants.

3.3.2 Scuffing Behaviour at 75 N

Figure 10 shows the friction coefficient during the test sequences at 75 N for the nine test lubricants. As at 20 N, all lubricant additives effectively extended scuffing life. At

this applied load, all the lubricants showed scuffing except for the two ZDDPs and TPP. The two concentrations of EP additive and also GMO scuffed at lower speeds at this load than they did 20 N. ZDDP1 and ZDDP2 gave relatively high fluctuations of friction coefficient similar to those seen at 20 N. MoDTC produced a very low friction coefficient of 0.05 until a sudden friction increase at 2 m/s, corresponding to scuffing.

Figure 11 shows the evolution of tribofilm thickness of the lubricants during the tests. ZDDP1, ZDDP2 and TPP formed relatively thick tribofilms of ca. 30 nm at 75 N, and these tribofilms presumably effectively protected the surfaces from scuffing up to 6 m/s sliding speed. The evolution of tribofilm thickness and SLIM images clearly show the continuous formation and removal of tribofilms of ZDDP2. DDP and MoDTC formed considerably thinner tribofilms at 75 N than at 20 N and the tribofilm formed by DDP shows an interesting progressive decline as the scuffing speed is approached. A similar steady loss of tribofilm prior to scuffing is also seen with the EP additive. GMO formed negligible tribofilm in the test stage. This might suggest that its ability to postpone scuffing results from its effect on friction as much as from its ability to separate surfaces. It is important to note that, as at 20 N, no significant distortion of circular shape in SLIM images of ZDDP2 caused by mild wear was observed at 75 N.

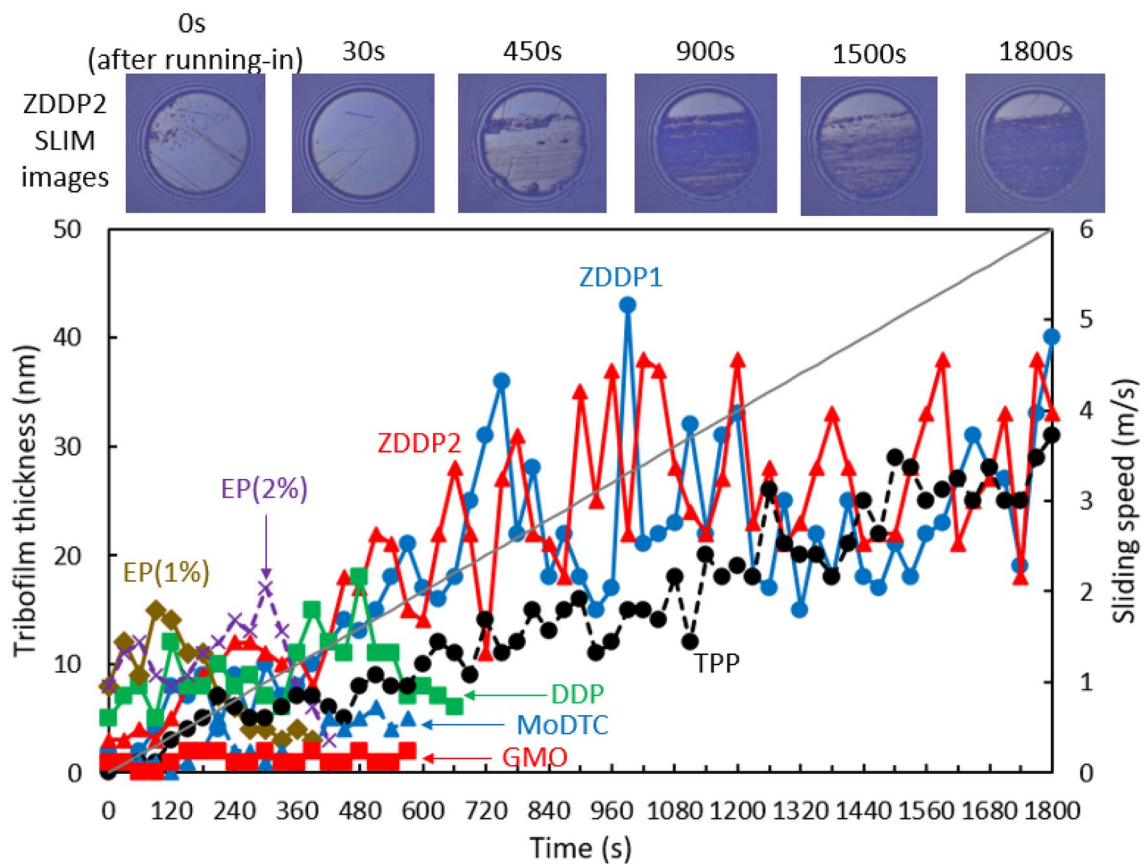


Fig. 11 The development of tribofilm thickness by eight additive solutions at 75 N as quantified by SLIM images captured during the rest stages. SLIM images of ZDDP2 at given durations are shown

3.3.3 Scuffing Behaviour at 570 N

Figure 12 shows how friction coefficient varied during the test stages at 570 N for the nine lubricants. At this load, all lubricants gave scuffing at a sliding speed test stage well below the maximum possible 6 m/s. Additive-free PAO scuffed at 0.4 m/s sliding speed, while MoDTC and OFM scuffed at a very low value of 0.5 m/s sliding speed. Unlike their behaviour at 20 N and 75 N, these additives did not show significantly lower friction coefficient than most other additives. EP(1%) and EP(2%) slightly extended scuffing life up to the 0.7 m/s sliding speed. A larger extension of scuffing life was observed in ZDDP1 and ZDDP2, to 1.3 m/s and 1.1 m/s of sliding speed, respectively.

Figure 13 shows the evolution of tribofilm thickness during the tests. MoDTC and GMO showed negligible tribofilm formation, consistent with their very low scuffing performance. DDP, EP(1%), EP(2%) and TPP formed tribofilms more than 20 nm thick after the initial, 0.1 m/s test stage. These tribofilms then progressively decreased in thickness as sliding speed increased, until scuffing occurred when their thickness declined below about 10 nm. This

decrease in thickness occurred much more rapidly for the EP additives than for DDP and TPP, so the latter showed more scuffing resistance. Based on the SLIM images of ZDDP2, a glassy film formed on some parts of the wear tracks during the running-in stage, but this tribofilm was then largely replaced by a 120 nm thick tribofilm with a fine appearance over the whole track. This tribofilm then progressively declined in thickness as the sliding speed was raised until scuffing occurred when the thickness fell below about 15 nm. Similar behaviour was observed for ZDDP1.

It should be noted that no significant distortion of a circular shape in the SLIM images of ZDDP2 caused by wear was observed even at 570 N up to the 0.9 m/s sliding speed tests stage. Above this, deep scratches across a wide area were observed. The circular shape was completely lost at the next stage of 1.1 m/s of sliding speed after scuffing occurred. This trend was seen for all lubricants.

3.4 Surface Observation

Figure 14 shows micrographs of the MTM discs and balls at the end of MoDTC solution tests at 20 N, 75 N and 570 N,

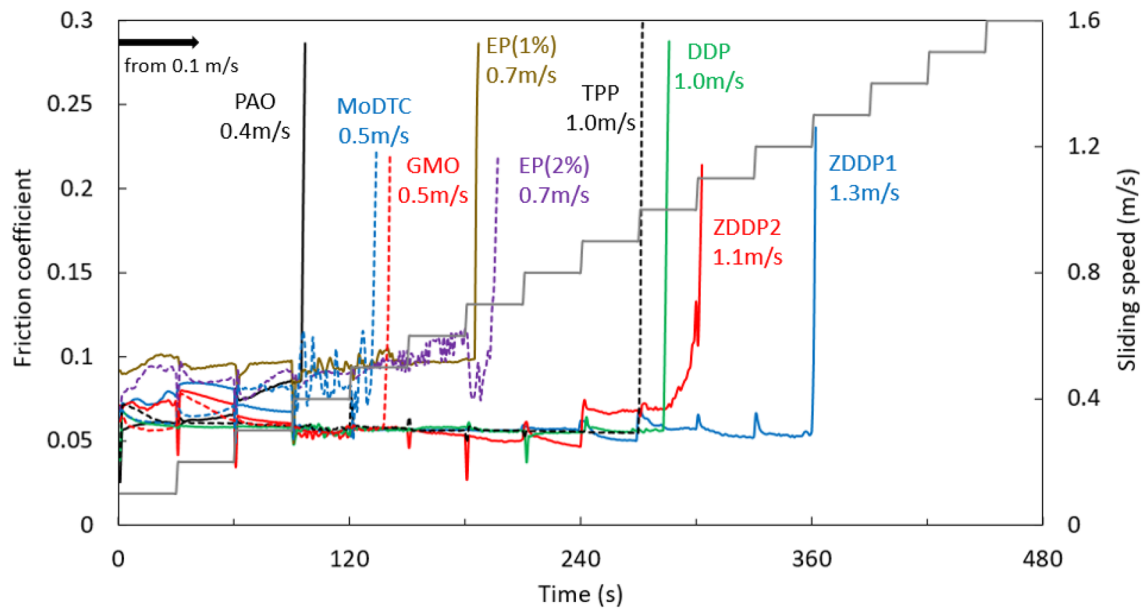


Fig. 12 The development of friction coefficient during the test stages at 570 N in the nine lubricants. Tests were carried out at the conditions shown in Table 2

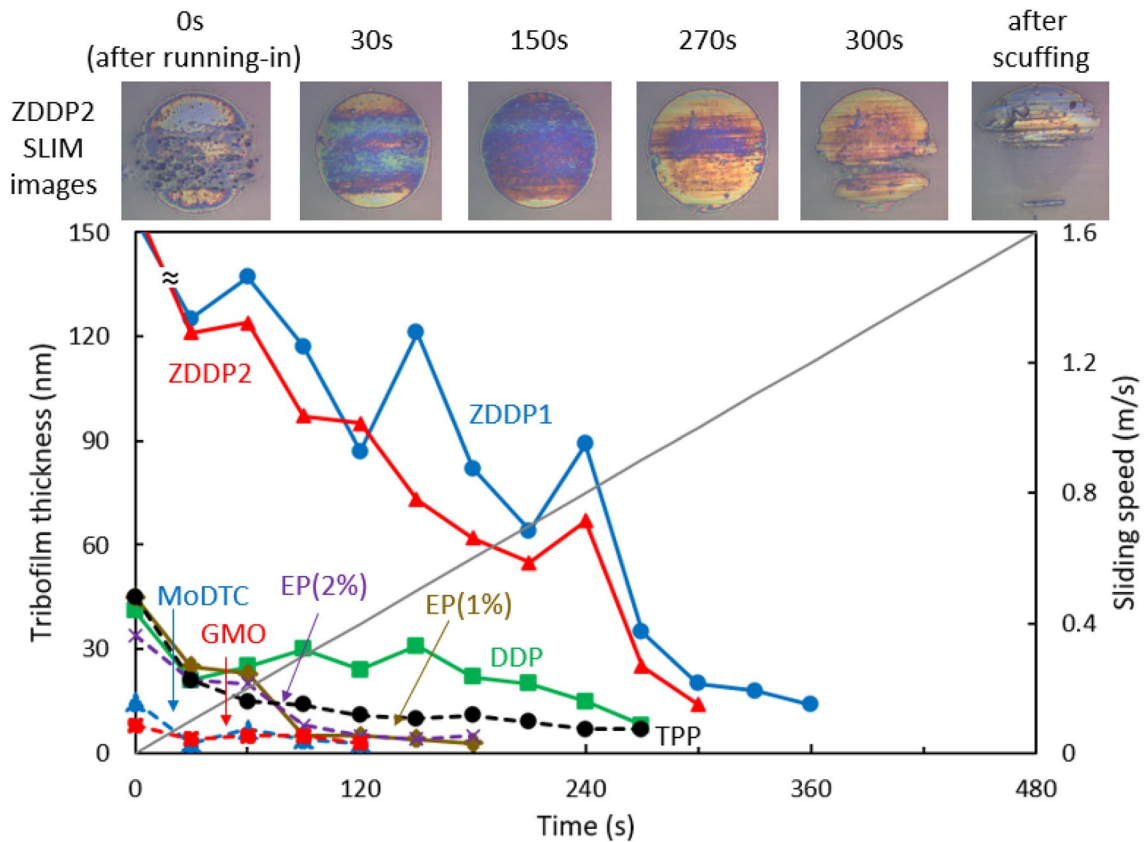


Fig. 13 The development of tribofilm thickness by eight additive solutions at 570 N as quantified by SLIM images captured during the rest stages. SLIM images of ZDDP2 at given durations are shown

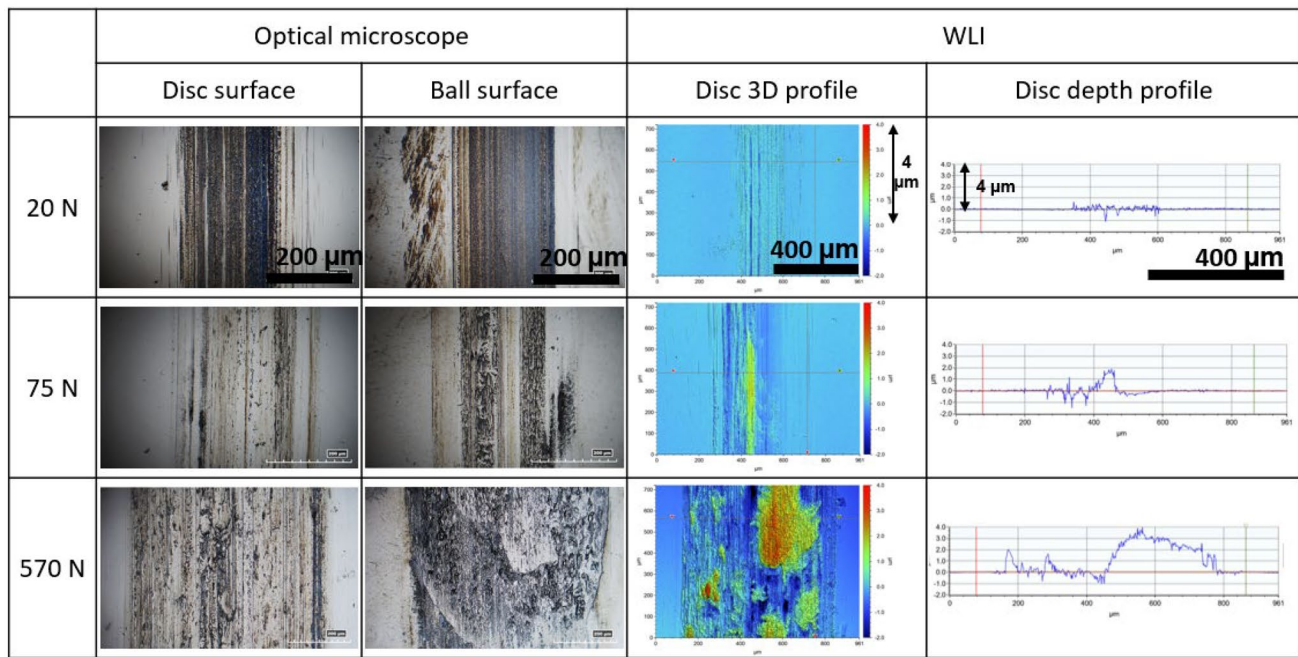


Fig. 14 Micrographs, 3D profiles and depth profiles of the surfaces of the test specimens after the completed tests at 20 N, 75 N and 570 N with an MoDTC oil. Note that the scales in the images at 20 N are applicable to the data at 75 N and 570 N

together with 3D profiles and depth profiles of the discs obtained using WLI. When scuffing did not occur at 20 N, the wear tracks of the disc and the ball after 6 m/s sliding speed were covered with dark and blue coloured tribofilms. WLI 3D and depth profiles did not show significant wear on the disc surface. By contrast, after 75 N and 570 N load tests in which scuffing occurred, the surfaces of both balls and discs had a torn appearance. WLI 3D and depth profiles of the discs showed that large amounts of material adhered to the disc surfaces, presumably detached from the counterpart ball surfaces. The amount of material adhered to the discs was dependent on the applied load, i.e. 570 N showed a larger amount of adhered material on the disc, with ca. 4 μm of maximum height, compared to 75 N with ca. 2 μm . This adhesive transfer is generally considered to be characteristic of scuffing damage in real components including gears, rolling bearings and cam-followers, indicating that the present test can successfully reproduce the phenomenon. Also, this contra-rotational method did not give significant cumulative mild wear on the surfaces before scuffing and should, thus, eliminate the effect of the reduction of contact pressure during tests and hence help to properly assess the scuffing performance of the lubricants.

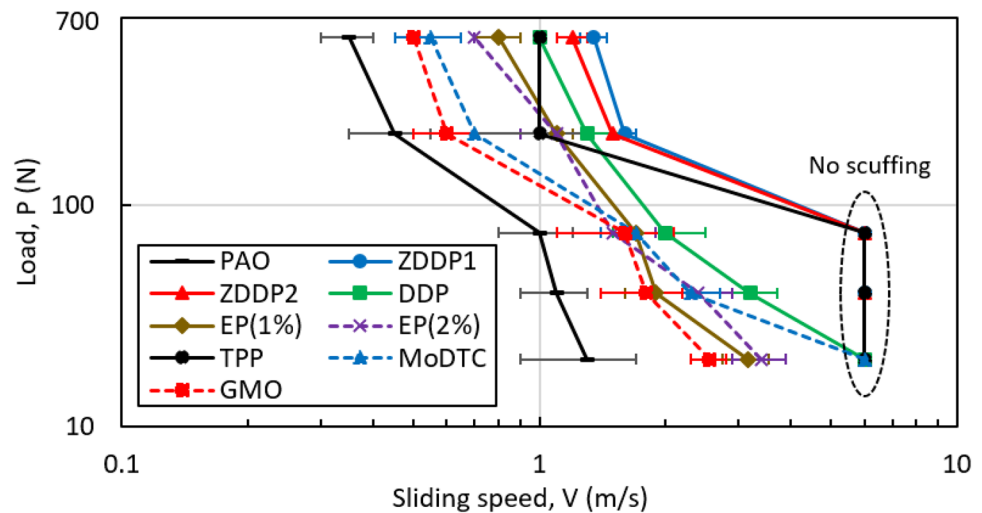
4 Discussion

4.1 Summary of Scuffing Behaviour of Lubricants

Transition diagrams in the form of load, P , versus sliding speed, U_s , charts can be used to define safe and unsafe operating regions for scuffing failure for a given oil–material combination [35, 36]. Such charts, often referred to as PV charts, have an obvious practical use in component design and lubricant selection. To illustrate the relative differences in scuffing performance of the lubricants used in the current study, Fig. 15 plots the results shown in Sect. 3.3 on a load versus sliding speed graph. The results obtained at 40 N and 210 N of load, corresponding to 1.0 GPa and 1.8 GPa maximum Hertzian contact pressure are included. The plotted scuffing speed for each lubricant is the average of at least three repeats at each load/lubricant combination condition. Error bars (based on the maximum and minimum values) are presented to indicate the spread of the scuffing speed data. Note that the points at 6 m/s show conditions at tests when scuffing did not occur.

It can be seen that scuffing becomes more likely as both load and sliding speed increase. All lubricant additives in PAO successfully alleviated scuffing to some extent, especially at low loads. In particular, ZDDPs and TPP, commonly used as antiwear additives, showed much better anti-scuffing performance than the other additives. Compared to these, EP(1%) and EP(2%) gave relatively poor scuffing

Fig. 15 Load versus sliding speed chart for the lubricants at given load using MTM and ETM. Note that the points at 6 m/s show conditions at tests when scuffing did not occur



performance. In the case of friction modifiers, while MoDTC prevented the outset of scuffing at 20 N, it did not effectively extend scuffing life at a higher load, whereas GMO did so.

The shape of the curves in Fig. 15 is indicative of a power law relationship where P is the load, (not contact pressure), U_s is the sliding speed and n is a constant.

$$PU_s^n = \text{constant} \quad (1)$$

Log(load) versus log(sliding speed) plots for all the oils confirmed the relationship $PU_s^n = \text{constant}$ at the onset of scuffing and enabled the values of the sliding speed exponent, n , to be calculated. ZDDPs and TPP were excluded since there were not enough data for n to be calculated reliably. Additive-free PAO gave a value of $n = 2.2$, which is in line with the values obtained by Peng et al. [15], i.e. 1.7 to 2.2 for base oils alone. The additive-containing lubricants gave a slightly higher value of ca. 2.5, suggesting that an additional mechanism is in play.

4.2 Scuffing and Tribofilm Development of AW, EP and FM Additives

The results obtained here suggest that the different classes of additive function in different ways to influence scuffing. Generally, antiwear and EP additives form tribofilms that prevent asperity contacts. Phosphorus-containing antiwear additives form relatively thick phosphate tribofilms [28, 37]. The test condition in Table 2 allows their solutions to form sufficient tribofilm at mild conditions before the critical sliding stage at which scuffing occurs. Consequently, these antiwear additives form relatively thick tribofilms that give an excellent improvement of anti-scuffing performance. Recently, Chern et al. [38] showed that enough running-in process in a ZDDP solution to form tribofilm effectively increased the scuffing load. By contrast, sulfur-based EP

additives react with ferrous surface under extreme conditions to form FeS and/or FeS_2 quite quickly [37, 39, 40]. These tribofilms protect against scuffing and welding although thicknesses are much thinner than those of phosphate tribofilms. In this study, interestingly, EP(1%) and EP(2%) gave scuffing at a relatively lower sliding speed than antiwear additives. To understand this behaviour, additional tests were carried out using initial sliding speed test stages of 0.6 m/s and 1 m/s.

Figure 16a, b compares friction development in 75 N tests with ZDDP2 and EP(2%) at different initial sliding speeds. With ZDDP2, initial sliding speeds of both 0.6 m/s and 1.0 m/s gave scuffing at 1.0 m/s. By contrast, at both these initial sliding speeds, EP(2%) scuffed at a higher sliding speed of around 1.6 m/s.

Figure 17 shows SLIM images and mean tribofilm thicknesses formed by EP(2%) after the running-in stage and after test stages at 0.1, 0.6, 0.9 and 1.4 m/s from separate tests starting at sliding speeds of 0.1, 0.6 and 1 m/s. EP(2%) formed a tribofilm thickness more than twice as thick as that of ZDDP2 after the running-in stage to reach a thickness greater than 10 nm after the 0.9 m/s sliding speed stage. This tribofilm then became very thin at 1.4 m/s sliding speed, and scuffing occurred at the next sliding stage of 1.5 m/s. This result shows that EP(2%) forms tribofilms fast enough to protect against scuffing around 1.0 m/s sliding speed, where scuffing occurs or the base oil. However, unlike ZDDP2, as rubbing progresses, these tribofilms do not grow further but instead thin down, resulting in scuffing at around 1.6 m/s sliding speed.

Unlike antiwear and EP additives, FMs reduced friction coefficient. Friction reduction by MoDTC is well known to originate from the formation of nanocrystals of low shear strength MoS_2 on rubbing asperities [41–44]. GMO forms films through physical and/or chemical adsorption rather than chemically reacted tribofilms, and such adsorbed films

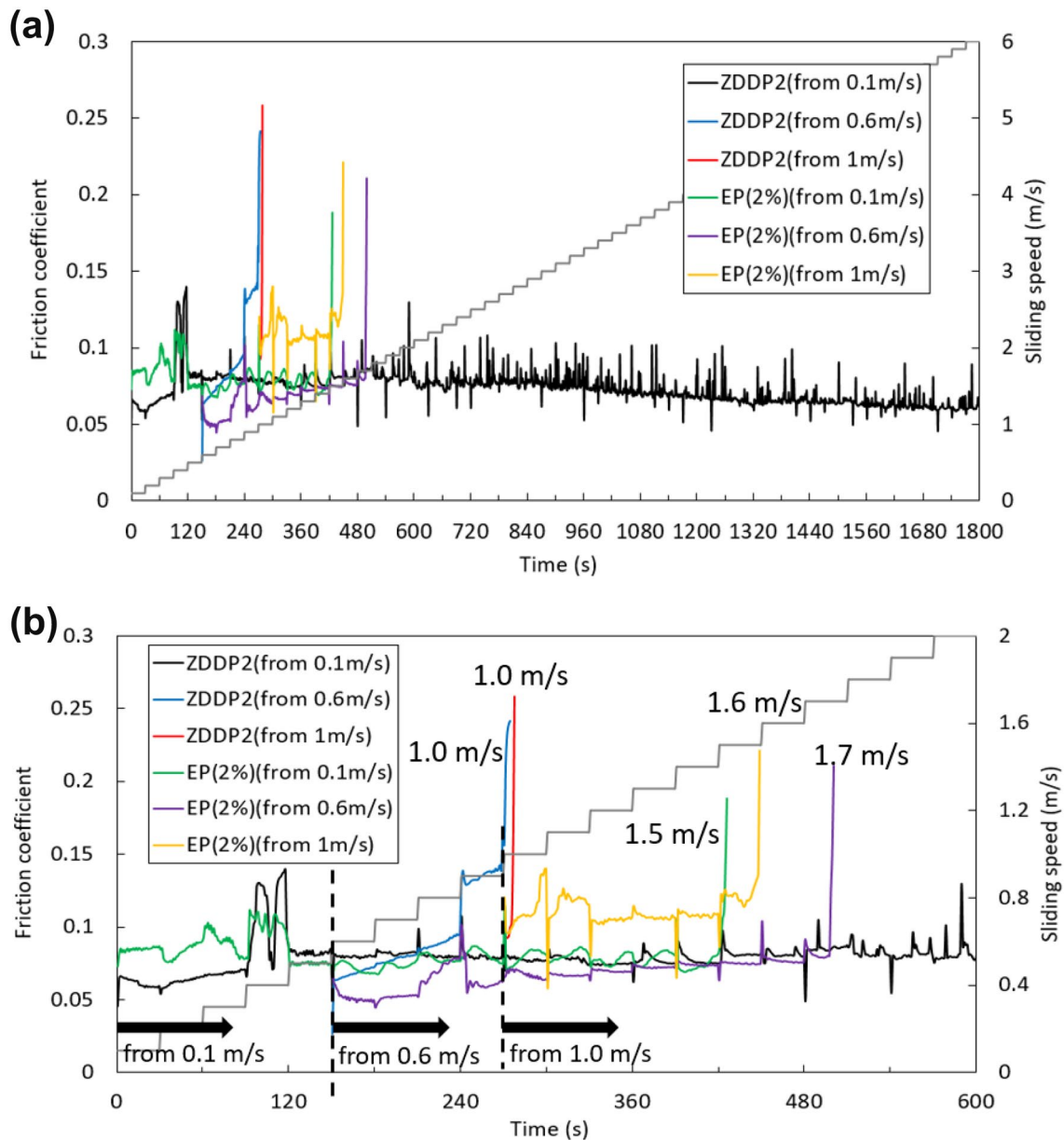


Fig. 16 The effect of initial sliding speed on friction coefficient in ZDDP2 and EP(2%) at 75 N. **a** shows the data from 0 to 6 m/s of sliding speed while **b** focusses on the friction data between 0 and 2 m/s.

are likely to be more easily removed [45]. Friction reduction lowers frictional heat in the contact and may suppress thinning down of oil film, which appears to result in some protection against scuffing. However, these FMs were found to reduce friction only at relatively low loads.

4.3 Scuffing Test Method Comparison

It is of interest to compare the scuffing properties of the lubricants using a four-ball EP test, which is traditionally used to study lubricant wear and scuffing performance of

Except the initial sliding speed in the test stage, the tests were carried out in the conditions shown in Table 2

lubricants. To do this, ASTM D 2783 tests were carried out on the nine test lubricants of this study. ASTM D 2783 is entitled “The Standard Test Method for Measurement of Extreme-Pressure Properties of Lubricating Fluids (Four-Ball Method)” and in this test, an upper ball is loaded and rotated against three lower, stationary balls. The rotating speed is 1760 ± 40 rpm. The temperature of lubricants is not controlled and tests are carried out at room temperature. Load is increased until welding occurs in a *step-load* sequence. Each load step has 10 s duration. After each load step, the test balls are replaced. Figure 18 shows the average





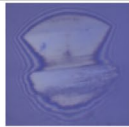





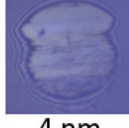
	after running-in	after 0.1 m/s	after 0.6 m/s	after 0.9 m/s	after 1.4 m/s
EP(2%) from 0.1 m/s	 8 nm	 11 nm	 11 nm	 13 nm	 3 nm
EP(2%) from 0.6 m/s	 9 nm	-	 13 nm	 13 nm	 3 nm
EP(2%) from 1 m/s	 8 nm	-	-	-	 4 nm

Fig. 17 The effect of initial sliding speed on tribofilm development of EP(2%) at 75 N. SLIM images after running-in and the given test stage are shown

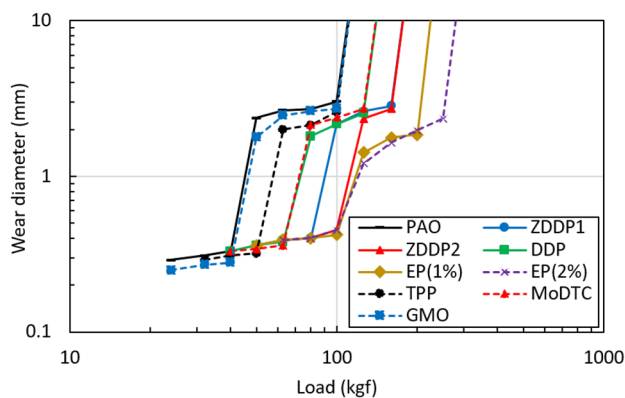


Fig. 18 EP properties of the lubricants using the four-ball EP test method (ASTM D 2783)

wear diameter on the three balls in the nine lubricants after each load step. Table 4 shows the last non-seizure load (LNL), initial seizure load (ISL), weld load (WL) and load wear index (LWI) obtained from Fig. 18. When scuffing occurs, a wear diameter suddenly increases at a given load. This load corresponds to ISL.

Unlike the results from the step-speed MTM and ETM tests described above, in the four-ball tests, EP(1%) and EP(2%) remarkably increase ISL and keep ball wear diameters at lower levels than the other lubricants after scuffing; i.e. the extent of scuffing damage in EP additives was less severe than the others. By comparison, TPP did not effectively protect against scuffing as it did in the speed-step

Table 4 Results of extreme-pressure properties of the lubricants using the four-ball EP method (ASTM D2783)

	Last non-seizure load (LNL)	Initial seizure load (ISL)	Weld load (WL)	Load wear index (LWI)
PAO	40	50	126	16.9
ZDDP1	80	100	200	34.3
ZDDP2	100	126	200	41.6
DDP	63	80	160	27.6
EP(1%)	100	126	250	48.4
EP(2%)	100	126	315	52.7
TPP	50	63	126	21.5
MoDTC	63	80	160	27.0
GMO	40	50	126	17.4

sequence. Similar to the results in the speed-step sequence, FMs gave relatively low scuffing load.

In the four-ball test, the key response needed for lubricants to extend scuffing life is to form tribofilms very quickly, within 10 s duration at high contact pressure. Sulphur-based EP additives react with surface quickly under extreme pressure to form FeS/FeS₂, resulting in an excellent protection against scuffing as well as welding [37, 39, 40]. By contrast, antiwear additives, especially ashless types, i.e. TPP and DDP, need a certain amount of rubbing time to form protective tribofilms and, hence, may not form thick protective tribofilms in the 10 s duration at high load.

It should be noted that this ability of EP additives to form tribofilms much more rapidly than P-based AW additives is

also likely to lead to a higher scuffing load in step-load tests, since in these tests, fresh surface without any tribofilm is introduced into contact at each load stage. An additive that can form a protective tribofilm on this surface very rapidly should show superior anti-scuffing performance.

Generally, in mechanical systems such as gears, bearings and cam-followers, surfaces are rubbed for relatively long duration, then suddenly scuffing occurs. This may occur from a sudden increase in load, a change in temperature, debris entering the contact or, indeed other, unknown changes in operating conditions. Based on this, there are possibly two aspects to protecting surfaces against scuffing by forming tribofilms. First, lubricants are desired to form thick and durable tribofilms, for example, phosphate tribofilms by antiwear additives, to protect surfaces under mild conditions. Second, when new asperities are introduced into contact and/or tribofilms are removed due to sudden increase of load or other condition, it is important to very quickly form protective tribofilms, for example the FeS/FeS₂ tribofilms from S-based EP additives. Therefore, in terms of lubricant formulation for such mechanical systems, a mixture of these two types of additive behaviour is the key technology to protect against scuffing. To study lubricant performance, test methods must be selected with care and insight.

5 Conclusions

In this study, the impact of various lubricant additives on scuffing was studied using a test method based on contra-rotation and a step-speed sequence implemented on MTM-SLIM and ETM-SLIM ball-on-disc tribometers. The results provide new understanding of the influence of tribofilm development on scuffing and suggest relevant mechanisms by which tribofilms mitigate scuffing. Key conclusions are as follows.

- The initial sliding speed in the step-speed sequence in scuffing tests significantly affects the scuffing performance of lubricants which contain tribofilm-forming additives. This is because tribofilm formation depends on sliding distance and if the test step-speed sequence starts at too high sliding speed, an effective tribofilm is unable to form before a critical scuffing speed is reached.
- ZDDPs, ashless P-additives and sulphur-based EP additive all show significant anti-scuffing performance.
- Generally, thicker tribofilms, especially those formed by ZDDPs and triphenyl phosphate, protect most effectively against scuffing. These tribofilms are progressively removed at high sliding speeds and scuffing then occurs when tribofilms become too thin to offer adequate protection and collapse.

- Unlike a step-speed sequence test using MTM and ETM, in the four-ball test, the key response needed for lubricants to extend scuffing life is to form tribofilms very quickly at high contact pressure as is the case for Sulphur-based EP additives.
- The insights presented here can help with the design of components and lubricants that are effective in controlling scuffing.

Acknowledgements The authors would like to thank Dr. Jie Zhang for his help in ETM scuffing tests.

Funding The authors declare that no funds, grants, or other support were received during the preparation of this manuscript.

Declarations

Competing Interests The authors declare that they have no conflict of interest.

Open Access This article is licensed under a Creative Commons Attribution 4.0 International License, which permits use, sharing, adaptation, distribution and reproduction in any medium or format, as long as you give appropriate credit to the original author(s) and the source, provide a link to the Creative Commons licence, and indicate if changes were made. The images or other third party material in this article are included in the article's Creative Commons licence, unless indicated otherwise in a credit line to the material. If material is not included in the article's Creative Commons licence and your intended use is not permitted by statutory regulation or exceeds the permitted use, you will need to obtain permission directly from the copyright holder. To view a copy of this licence, visit <http://creativecommons.org/licenses/by/4.0/>.

References

1. Dyson, A.: Scuffing—a review. *Tribol. Int.* **8**, 77–87 (1975)
2. Bowman, W.F., Stachowiak, G.W.: A review of scuffing models. *Tribol. Lett.* **2**, 113–131 (1996)
3. Braun, H.R., Korres, S., Laurs, P., Franke, J.W.H.: Impact of ultra-low viscosity fluids on drivetrain functionality and durability. *Lubricants* **9**, 119 (2021)
4. Li, S., Kolivand, A., Wei, J.: Determination of critical temperature of scuffing for AISI 8620 steel gear contacts lubricated by dexron 6 through computational simulation of experiment. *J. Tribol.* **144**, 081201 (2022)
5. Schipper, D.J., De Gee, A.W.J.: Lubrication modes and the IRG transition diagram. *Lubr. Sci.* **8**, 27–35 (1995)
6. Yagi, K., Izumi, T., Koyamachi, J., Sanda, S., Yamaguchi, S., Satio, K., Tohyama, M., Sugimura, J.: In situ observation of crystal grain orientation during scuffing process of steel surface using synchrotron X-ray diffraction. *Tribol. Lett.* **68**, 1–15 (2020)
7. Snidle, R.W., Rossides, S.D., Dyson, A.: The failure of elastohydrodynamic lubrication. *Proc. R. Soc. Lond. A* **395**, 291–311 (1984)
8. Li, S., Kahraman, A., Anderson, N., Wedeven, L.D.: A model to predict scuffing failures of a ball-on-disk contact. *Tribol. Int.* **60**, 233–245 (2013)

9. Castro, J., Seabra, J.: Scuffing and lubricant film breakdown in FZG gears part I. Analytical and experimental approach. *Wear* **215**, 104–113 (1998)
10. Forbes, E.: Antiwear and extreme pressure additives for lubricants. *Tribol. Int.* **3**, 145–152 (1970)
11. Piekoszewski, W., Szczerek, M., Tuszyński, W.: The action of lubricants under extreme pressure conditions in a modified. *Wear* **249**, 188–193 (2001)
12. Yamamoto, Y., Hirano, F.: Scuffing resistance of phosphate esters. *Wear* **50**, 343–348 (1978)
13. Palacios, J.M.: Films formed by antiwear additives and their incidence in wear and scuffing. *Wear* **114**, 41–49 (1987)
14. Miyajima, M., Kitamura, K., Matsumoto, K.: In Situ raman tribometry for the formation and removal behavior of FeS₂ tribofilm in the scuffing process. *Tribol. Online* **11**, 382–388 (2016)
15. Peng, B., Spikes, H., Kadiric, A.: The development and application of a scuffing test based on contra-rotation. *Tribol. Lett.* **67**, 1–25 (2019)
16. Bayat, R., Lehtovaara, A.: Scuffing evaluation of fully formulated environmentally acceptable lubricant using barrel-on-disc technique. *Tribol. Int.* **160**, 107002 (2021)
17. Ingram, M., Hamer, C., Spikes, H.: A new scuffing test using contra-rotation. *Wear* **328–329**, 229–240 (2015)
18. Hersberger, J., Ajayi, O.O., Zhang, J., Yoon, H., Fenske, G.R.: Evidence of scuffing initiation by adiabatic shear instability. *Wear* **258**, 1471–1478 (2005)
19. Ludema, K.C.: A review of scuffing and running-in of lubricated surfaces, with asperities and oxides in perspective. *Wear* **100**, 315–331 (1984)
20. Ajayi, O.O., Hersberger, J.G., Zhang, J., Yoon, H., Fenske, G.R.: Microstructural evolution during scuffing of hardened 4340 steel—implication for scuffing mechanism. *Tribol. Int.* **38**, 277–282 (2005)
21. Yoon, H., Zhang, J., Kelley, F.: Scuffing characteristics of sae 50b38 steel under lubricated conditions. *Tribol. Trans.* **45**, 246–252 (2002)
22. Bisht, R.P.S., Singhal, S.: A laboratory technique for the evaluation of automotive gear oils of API GL-4 level. *Tribotest* **6**, 69–77 (1999)
23. Ku, P.M., Baber, B.B.: The effect of lubricants on gear tooth scuffing. *ASLE Trans.* **2**, 184–194 (1959)
24. Zaskal'ko, P.P., Kuznetsov, E.G., Krysin, V.D., Chechetkin, V.V.: Evaluation of antiscuff properties of transmission oils in IAE tester by qualification test procedure. *Chem. Technol. Fuels Oils* **12**, 556–559 (1967)
25. Perez, J.M., Weller, D.E., Duda, J.L.: Sequential four-ball study of some lubricating oils. *Lubr. Eng.* **55**, 28–32 (1999)
26. Cann, P.M., Spikes, H.A., Hutchinson, J.: The development of a spacer layer imaging method (slim) for mapping elastohydrodynamic contacts. *Tribol. Trans.* **39**, 915–921 (1996)
27. Enthoven, J., Spikes, H.A.: Infrared and visual study of the mechanisms of scuffing. *Tribol. Trans.* **39**, 441–447 (1996)
28. Spikes, H.: The history and mechanisms of ZDDP. *Tribol. Lett.* **17**, 469–489 (2004)
29. Ueda, M., Kadiric, A., Spikes, H.A.: On the crystallinity and durability of ZDDP tribofilm. *Tribol. Lett.* **67**, 1–13 (2019)
30. Ueda, M., Kadiric, A., Spikes, H.: Influence of steel surface composition on ZDDP tribofilm growth using ion implantation. *Tribol. Lett.* **69**, 62 (2021)
31. Ueda, M., Kadiric, A., Spikes, H.: ZDDP tribofilm formation on non-ferrous surfaces. *Tribol. Online* **15**, 318–331 (2020)
32. Pagkalis, K., Spikes, H., Jelita-rydel, J., Ingram, M., Kadiric, A.: The influence of steel composition on the formation and effectiveness of anti-wear films in tribological contacts. *Tribol. Lett.* **69**, 1–20 (2021)
33. Dawczyk, J., Morgan, N., Russo, J., Spikes, H.: Film thickness and friction of ZDDP tribofilms. *Tribol. Lett.* **67**, 34 (2019)
34. Zhang, J., Ueda, M., Campen, S., Spikes, H.: Boundary friction of ZDDP tribofilms. *Tribol. Lett.* **69**, 1–17 (2021)
35. Borsoff, V.N., Godet, M.R.: A scoring factor for gears. *ASLE Trans.* **6**, 147–153 (1963)
36. Cutiongco, E.C., Chung, Y.W.: Prediction of scuffing failure based on competitive kinetics of oxide formation and removal: application to lubricated sliding of AISI 52100 steel on steel. *Tribol. Trans.* **37**, 622–628 (1994)
37. Spikes, H.: Low- and zero-sulphated ash, phosphorus and sulphur anti-wear additives for engine oils. *Lubr. Sci.* **20**, 103–136 (2008)
38. Chern, S.Y., Ta, T.N., Horng, J.H., Wu, Y.S.: Wear and vibration behavior of ZDDP-containing oil considering scuffing failure. *Wear* **478–479**, 203923 (2021)
39. Spikes, H.A., Cameron, A.: Additive interference in dibenzyl disulfide extreme pressure lubrication. *ASLE Trans.* **17**, 283–289 (1974)
40. Najman, M.N., Kasrai, M., Bancroft, G.M.: X-ray absorption spectroscopy and atomic force microscopy of films generated from organosulfur extreme-pressure (EP) oil additives. *Tribol. Lett.* **14**, 225–235 (2003)
41. Feng, I.M., Perilstein, W.L., Adams, M.R.: Solid film deposition and non-sacrificial boundary lubrication. *ASLE Trans.* **6**, 60–66 (1963)
42. Grossiord, C., Varlot, K., Martin, J., Le Mogne, T., Esnouf, C.: MoS₂ single sheet lubrication by molybdenum. *Tribol. Int.* **31**, 737–743 (1999)
43. Ueda, M., Kadiric, A., Spikes, H.: Wear of hydrogenated DLC in MoDTC-containing oils. *Wear* **474–475**, 203869 (2021)
44. Ueda, M., Wainwright, B., Spikes, H., Kadiric, A.: The effect of friction on micropitting. *Wear* **488–489**, 204130 (2022)
45. Spikes, H.: Friction modifier additives. *Tribol. Lett.* **60**, 5 (2015)

Publisher's Note Springer Nature remains neutral with regard to jurisdictional claims in published maps and institutional affiliations.